



Yu, L. and Chan, Tommy H. and Zhu, J.H. (2008) Moving vehicle load identification from bridge responses based on method of moments (MOM) . In Jacob, B. and O'Brien, E. and O'Connor, A. and Bouteldja, M., Eds. *Proceedings International Conference on Heavy Vehicles Paris 2008 incorporating Heavy Vehicle Transport Technology (HVTT 10) and Weigh-In-Motion (ICWIM 5)*, pages pp. 297-310, Paris, France.

© Copyright 2008 International Forum for Road Transport Technology (IFRTT)

# MOVING VEHICLE LOAD IDENTIFICATION FROM BRIDGE RESPONSES BASED ON METHOD OF MOMENTS (MOM)



L. YU<sup>1,3</sup>

<sup>1</sup> Dept of Mechanics & Civil Eng.  
Jinan University,  
Guangzhou, 510632, P. R. China



T. H. T. CHAN

<sup>2</sup> School of Urban Development  
Queensland University of Technology,  
Brisbane, Queensland 4001, Australia



J. H. ZHU<sup>1,3</sup>

<sup>3</sup> Key Lab of Geo. Mechanics & Eng.  
Changjiang River Sci. Res. Inst.,  
Wuhan, 430010, P. R. China

## Abstract

A MOM-based algorithm (MOMA) is proposed for identifying of the time-varying moving vehicle loads on a bridge in this paper. A series of numerical simulations and experiments in laboratory have been studied and the proposed MOMA are compared with the existing time domain method (TDM). A few main parameters, such as basis function terms, executive CPU time, Nyquist fraction of digital filter, two different solutions to the ill-posed system equation, etc, have been investigated. Both the numerical simulation and experimental results show that the MOMA has higher identification accuracy and robust noise immunity as well as producing an acceptable solution to ill-conditioning cases to some extent, but its CPU execution time is just less than one tenth of the TDM.

**Keywords:** Moving force identification, Method of moments (MOM), Bridge-vehicle interaction

## 1. Introduction

The study of moving vehicle loads on a bridge deck is an important issue from the aspects of design, diagnosis and maintenance of bridges, as they contribute to the live load component in a bridge design code (Ting, 1983). Direct measurements of the forces using instrumented vehicles are expensive and are subjected to bias (Cantineni, 1992, Heywood, 1994). Some systems have been developed for so called ‘weigh-in-motion’ of vehicles (Peters, 1984 & 1986), but they all measure only the equivalent static axle loads. It has been observed that the induced dynamic deflection and stresses can be a significantly higher than those observed in the static case as a structure is subjected to moving loads, for example, a dynamic increment of 125% was obtained on a small composite bridge (Chan, 1990).

In the last decade, a few indirect identification methods were successively proposed and incorporated into a moving force identification system (MFIS) (Yu & Chan, 2002). Numerical simulations, illustrative examples and comparative studies show that each method involved in the MFIS could effectively identify moving forces with acceptable accuracy (Chan & Yu, 2001), both time domain method (TDM) and frequency time domain method (FTDM) were found better than others (Yu & Chan, 2002 & 2007). However, there still exist some limitations if these methods could actually be operated in practice.

Based on the Method of moment (MOM) and the theory of moving force identification, a MOM-based algorithm (MOMA) is proposed for identifying the dynamic axle loads with the aim to overcome the limitations induced from the ill-conditioned problem. The moving vehicles loads were described as a combination of whole basis functions, and further were estimated by solving the new system equations developed with the basis functions. Compared with the existing time domain method (TDM), the illustrated results show that the MOMA has higher identification accuracy, less noise sensitive and an acceptable solution to the ill-conditioned problem to some extent when the basis functions number were adopted properly. To further evaluate and critically investigate the MOMA, a series of experiments have been conducted for moving force identification under different conditions. In contrast to the TDM, a carefully comparative study scheme was planned and conducted, some conclusions finally made.

## 2. Basic Theory

### 2.1 Motion Equation of Bridge-vehicle System

A bridge superstructure is modeled as a simply supported beam as shown in Figure 1. The effects of shear deformation and rotary inertia are not taken into account (Bernoulli-Euler beam). If the dynamic vehicle load  $f(t)$  moves from left to right at a speed  $c$ , then an equation of motion in terms of modal coordinate  $q_n(t)$  can be expressed as

$$\ddot{q}_n(t) + 2\xi_n\omega_n\dot{q}_n(t) + \omega_n^2q_n(t) = \frac{2}{\rho L}p_n(t) \quad (n = 1, 2, \dots, \infty) \quad (1)$$

where

$$\omega_n = \frac{n^2\pi^2}{L^2}\sqrt{EI}, \xi_n = \frac{C}{2\rho\omega_n}, p_n(t) = f(t) \cdot \sin\frac{n\pi ct}{L} \quad (2)$$

They are the  $n$ th modal frequency, the modal damping ratio and the modal load,

respectively.  $\rho$  and  $L$  are the constant mass per unit length and the span length of bridge respectively.  $C$  is the proportional damping. The moving load identification is an inverse problem in structural dynamics, in which the unknown time-varying load  $f(t)$  can be identified from measured displacements, accelerations or bending moments of real structures.

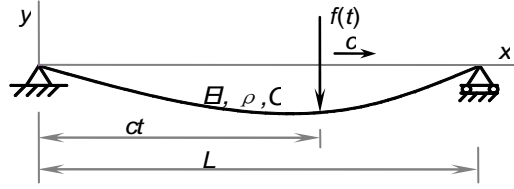


**Figure 1 - Moving load model**

Equation (1) can be solved in the time domain by the convolution integral and the dynamic deflection  $v(x, t)$  of the beam at point  $x$  and time  $t$  can be obtained as

$$v(x, t) = \sum_{n=1}^{\infty} \frac{2}{\rho L \omega_n'} \sin \frac{n\pi x}{L} \times \int_0^t e^{-\xi_n \omega_n (t-\tau)} \sin \omega_n' (t-\tau) \sin \frac{n\pi c\tau}{L} f(\tau) d\tau \quad (3)$$

Where  $\omega_n' = \omega_n \sqrt{1 - \xi_n^2}$ .

## 2.2 Moving Force Identification Based on Method of Moments (MOM)

The method of moments is based on the radical idea that the functional equation is rewritten in discrete terms. Assuming the dynamic vehicle load  $f(t)$  can be expressed as follows in terms of a series of basis function  $\psi_0(t), \psi_1(t), \psi_2(t), \dots, \psi_n(t)$  (Harrington, 1968).

$$f(t) = \sum_k \alpha_k \psi_k(t) \quad (4)$$

Arranging Equation (4) into a matrix form

$$f = \Psi \cdot \alpha \quad (5)$$

Where  $\psi_k(t) = P_k(t)$  (Jorgensen, 2004) or  $\psi_k(t) = \sin(k\pi ct/L)$  are the cases, while the basis functions are Legendre polynomials or Fourier series.

## 2.3 Identification from Bending Moment Responses and /or Acceleration Responses

The bending moment of the beam at point  $x$  and time  $t$  is

$$m(x, t) = -EI \frac{\partial^2 v(x, t)}{\partial x^2} = \sum_{n=1}^{\infty} \frac{2EI\pi^2}{\rho L^3} \frac{n^2}{\omega_n'} \sin \frac{n\pi x}{L} \times \int_0^t e^{-\xi_n \omega_n (t-\tau)} \sin \omega_n' (t-\tau) \sin \frac{n\pi c\tau}{L} f(\tau) d\tau \quad (6)$$

Letting the test function  $\omega_j = \delta(t - t_j)$ , substituting Equation (4) into Equation (6), multiplying by  $\omega_j$ , integrating the resultant equation with respect to time  $t$  between 0 and infinite, and using the properties of the test function  $\omega_j$ , Equation (6) can be then expressed as

$$m(x, t_j) = \sum_{k=0}^m \alpha_k \cdot l_{jk} \quad (j = 0, 1, \dots, N) \quad (7)$$

$$l_{jk} = \sum_{n=1}^{\infty} \frac{2EI\pi^2}{\rho L^3} \frac{n^2}{\omega_n'} \sin \frac{n\pi x}{L} \times \int_0^{t_j} e^{-\xi_n \omega_n (t_j-\tau)} \sin \omega_n' (t_j - \tau) \sin \frac{n\pi c\tau}{L} \psi_k(\tau) d\tau \quad (8)$$

where, the superscript  $m$  is the basis function number,  $t_j = j\Delta t$ ,  $\Delta t$  is the sampling interval and  $N$  the number of sample points for the measured bending moment responses.

Equations (7) and (8) can be rewritten in discrete terms and rearranged into a set of equations

$$M_{(N-1) \times 1} = L_{(N-1) \times (m+1)} \cdot \alpha_{(m+1) \times 1} \quad (9)$$

$$L_{(N-1) \times (m+1)} = B_{(N-1) \times (N_B-1)} \cdot \Psi_{(N_B-1) \times (m+1)} \quad (10)$$

where the  $\Psi$ ,  $M$  and  $\alpha$  are the matrix of basis functions, the time-series vector of the measured bending moment responses and the coefficient vector, respectively.

If  $N-1=m+1$ , the coefficient  $\alpha$  can be obtained directly by solving Equation (9). If  $N-1>m+1$  or  $N-1<m+1$ , the least-squares method can be used to find the coefficient  $\alpha$ . Substituting  $\alpha$  into Equation (5), the time history of the moving loads can be obtained finally.

If the acceleration at point  $x$  and time  $t$  is measured, a set of equations can be developed in a similar way as equations (9)-(10). The coefficient  $\alpha$  can be calculated by solving the similar equations, and then substituting  $\alpha$  into Equation (5), the load vector  $f$  can be obtained.

If the bending moments and the acceleration responses are measured at the same time, both of them can be used together to identify the moving load. The bending moment vectors  $M$  in Equation (9) and the acceleration vectors  $\ddot{v}$  should be first scaled to dimensionless units, and then the two equations can be combined, to yield

$$\begin{bmatrix} L/\|M\| \\ H/\|\ddot{v}\| \end{bmatrix} \cdot \alpha = \begin{Bmatrix} M/\|M\| \\ \ddot{v}/\|\ddot{v}\| \end{Bmatrix} \quad (11)$$

Where  $\|\bullet\|$  is the norm of a vector.

The above procedure is derived for the identification of a single load. It can be modified for the identification of multiple loads based on the linear superposition principle. It is easy to see that both the MOMA and the TDM will usually result in a system of equation, which can be solved by SVD and Tikhonov regularization methods respectively in this paper.

### 3. Numerical Simulation

#### 3.1 Bridge-vehicle and Simulation Parameters Considered

In order to check the correctness and effectiveness of the proposed method, the following identification of two moving vehicle loads is simulated and illustrated.

(i) Constant loads

$$f_1(t) = 58\,800 \text{ N}$$

$$f_2(t) = 137\,200 \text{ N}$$

$$l_s = 8 \text{ m}$$

(ii) Time-varying loads

$$f_1(t) = 58\,800 \times [1 + 0.1 \sin(10\pi t) + 0.05 \sin(40\pi t)] \text{ N}$$

$$f_2(t) = 137\,200 \times [1 - 0.1 \sin(10\pi t) + 0.05 \sin(50\pi t)] \text{ N}$$

$$l_s = 8 \text{ m}$$

The parameters of the beam bridge are as follows:  $EI = 1.27914 \times 10^{11} \text{ N}\cdot\text{m}^2$ ,  $\rho = 12\,000 \text{ kg/m}$ ,  $L = 40 \text{ m}$ ,  $f_1 = 3.2 \text{ Hz}$ ,  $f_2 = 12.8 \text{ Hz}$ ,  $f_3 = 28.8 \text{ Hz}$ . The moving speed  $c = 40 \text{ m/s}$ . the analysis frequency bandwidth is from 0 to 40 Hz and therefore the first three modes of the beam are included in the calculation. The sampling frequency  $f_s$  is 200 Hz. Random noise is added to the calculated responses to simulate the polluted measurements as one in Ref (Yu 2002).

The Fourier basis functions are only adopted for the MOMA in the following simulation studies because they enable the MOMA to have higher computation efficiency. The MOMA are used to identify both the two axle constant and time-varying loads from bending moment and/or acceleration responses at 1/4, 1/2, and 3/4 spans in twelve combination cases. Table 1 shows the comparison on the RQPE values of two axle constant loads identified by both the TDM and MOMA under the 5% noise level as well as including the effect of two different solutions, i.e. the SVD and regularization solutions. Selecting four out of twelve combination cases, Table 2 gives the comparison on the RQPE values of two axle time-varying loads

identified by TDM and MOMA when the SVD solution is adopted only. In addition, the effect of different noise levels on the RQPE values are also considered in Table 2. From Tables 1 and 2, some conclusions can be made as follows.

**Table 1** - Comparison on RQPE of two axle constant loads under 5% Noise

Sensor Location	TDM		MOMA					
	Axle 1	Axle 2	Axle 1	Axle 2				
1/4m&2/4m	*	<u>36.5</u>	*	<u>28.5</u>	1.06	<u>0.76</u>	0.25	<u>0.05</u>
1/4m&2/4m&3/4m	*	<u>34.4</u>	*	<u>27.6</u>	0.79	<u>0.39</u>	0.37	<u>0.04</u>
1/4a&2/4a	55.8	<u>14.1</u>	25.8	<u>10.9</u>	0.18	<u>0.18</u>	0.24	<u>0.24</u>
1/4a&2/4a&3/4a	2.58	<u>2.58</u>	1.40	<u>1.40</u>	0.10	<u>0.10</u>	0.21	<u>0.21</u>
2/4m&2/4a	*	<u>35.0</u>	*	<u>24.6</u>	0.26	<u>0.26</u>	0.15	<u>0.15</u>
1/4m&2/4m&2/4a	*	<u>25.2</u>	*	<u>23.2</u>	0.13	<u>0.13</u>	0.11	<u>0.11</u>
1/4m&2/4m&1/4a&2/4a	55.0	<u>16.6</u>	25.9	<u>10.8</u>	0.04	<u>0.04</u>	0.18	<u>0.18</u>
1/4m&1/4a	*	<u>28.2</u>	*	<u>23.5</u>	0.17	<u>0.17</u>	0.20	<u>0.20</u>
1/4m&1/4a&2/4a	62.8	<u>14.6</u>	28.2	<u>11.9</u>	0.25	<u>0.25</u>	0.20	<u>0.20</u>
2/4m&1/4a	*	<u>38.9</u>	*	<u>25.5</u>	0.41	<u>0.41</u>	0.18	<u>0.18</u>
1/4m&2/4m&1/4a	*	<u>29.8</u>	*	<u>22.2</u>	0.23	<u>0.23</u>	0.13	<u>0.13</u>
1/4a&2/4a&2/4m	53.2	<u>16.6</u>	24.9	<u>10.2</u>	0.14	<u>0.14</u>	0.22	<u>0.22</u>

Notes: \* indicates the error exceeds 100%, the underlined values are for regularization solution, and others for SVD solution.

**Table 2** - Comparison on RQPE of two axle time-varying loads identified via SVD

Sensor Location	1% Noise		5% Noise		10% Noise	
	Axle 1	Axle 2	Axle 1	Axle 2	Axle 1	Axle 2
1/4m&2/4m&3/4m	97.8	55.4	*	*	*	*
	<u>7.35</u>	<u>1.81</u>	<u>36.7</u>	<u>9.03</u>	<u>73.5</u>	<u>18.1</u>
1/4m&2/4m&2/4a	*	29.6	*	*	*	*
	<u>4.45</u>	<u>1.50</u>	<u>22.3</u>	<u>7.50</u>	<u>44.5</u>	<u>15.0</u>
1/4m&1/4a&2/4a	31.5	22.1	*	*	*	*
	<u>1.31</u>	<u>0.76</u>	<u>6.54</u>	<u>3.81</u>	<u>13.1</u>	<u>7.62</u>
1/4a&2/4a&3/4a	0.93	0.63	4.66	3.13	9.30	6.25
	<u>0.86</u>	<u>0.31</u>	<u>4.29</u>	<u>1.56</u>	<u>8.58</u>	<u>3.11</u>

Notes: \* indicates the RQPE values exceeds 100%, the underlined values are for MOMA, and others for TDM.

(1) For any of cases in both Table 1 and 2, the MOMA results are obviously better than the TDM results whether for two constant load or for two time-varying load identification. For the cases of two axle constant load identification, the RQPE values by the MOMA are very low and less than 1.06% for all twelve cases in Table 1. They are dramatically lower than the RQPE values by the TDM. It shows that the MOMA is a very good identification method, which is especially suitable for two axle constant load identification.

(2) Compared the SVD results with the regularization results, it can be found from Table 1 that the RQPE values for all cases, except for the case of 1/4a&1/2a&3/4a, are significantly reduced if the regularization solution are adopted instead of the SVD solution for the TDM. For the MOMA, the RQPE values are also significantly improved when the bending moment responses are only used to identify the two moving loads. However, when only the acceleration responses, or the combination of acceleration and bending moment responses are used to identify the two moving loads, the RQPE values are close to each other whether the SVD or the regularization solution is adopted.

(3) For case comparison, Table 1 also shows that, the more the measurement station is, or the more the number of measured acceleration involved is, the better the identified results are. It shows that adopting more responses for two moving load identification is beneficial to both the TDM and the MOMA. From Table 2, it can be seen that the more the number of bending moment responses replaced with acceleration responses is, the better both the TDM and the MOMA results are. The best sensor arrangement is when all three sensors are accelerometers, i.e.  $1/4a$  &  $1/2a$  &  $3/4a$ , for both the two methods.

(4) It can also be found from Table 2 that the RQPE values are almost proportional to the noise levels. Obviously, the MOMA identification accuracy is higher than the TDM accuracy for each case. It shows that the MOMA immunity to the noise is higher than the TDM immunity when 1%, 5% and 10% noise were added into the responses. In other words, the proposed MOMA method is more suitable for identification of moving loads from the measured response signals contaminated by measurement noise.

#### 4. Experiments in Laboratory

After the identification accuracy of the proposed method had been evaluated through illustrative numerical simulation, a series of experiments were further conducted in laboratory for assessing the robustness of MOMA.

##### 4.1 Experimental setup

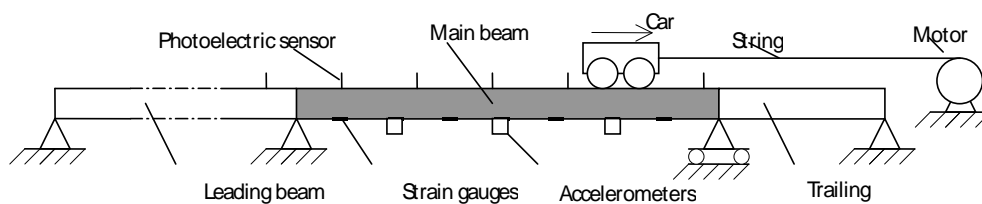


**Figure 2 - Experimental setup**

Both the model car and model bridge deck were constructed in the laboratory as shown in Figure 2. Here, the model car had two axles at a spacing of 0.55m and was mounted on four rubber wheels. The static mass of the whole vehicle was 12.1kg in which the mass of the rear wheel was 3.825kg. The model bridge deck consisted of a main beam, a leading beam and a trailing beam. The main beam, with a span of 3.678m long and a 101mm×25mm uniform cross section, was simply supported. It was made from a solid rectangular mild steel bar with a density of 7335kg/m<sup>3</sup> and a flexural stiffness  $EI=29.97\text{kN}\cdot\text{m}^2$ . Seven equally spaced strain gauges and three equally spaced accelerometers were mounted on the lower surface of the main beam to measure the bridge response due to the model car moving across it. The sampling frequency is 1000Hz for all the cases. Before exporting the measured data in ASCII format for identification, the Bessel IIR digital filter with low-pass characteristics was implemented as cascaded second order systems.

##### 4.2 Comparative Studies

The moving force identification includes many parameters, which are the critical parts in the identification processing. The comparative study is to investigate the effects of several

main parameters on the MOMA, and further compared with the existing TDM.

#### 4.2.1 Accuracy assessment

The identification accuracy of moving forces, called relative percentage error (RPE), is assessed indirectly through the measured and rebuilt responses as below:

$$RPE = \frac{\sum |R_{measured} - R_{rebuilt}|}{\sum |R_{measured}|} \times 100 \% \quad (12)$$

Here,  $R_{measured}$  and  $R_{rebuilt}$  indicate the measured and the rebuilt response respectively.

#### 4.2.2 Effect of basis function terms

Basis function plays an important role in the identification of moving loads for the MOMA. To assess the effect of basis function number ( $BFN$ ) on the MOMA, the other parameters are as following: the mode number of the bridge involved  $MN = 4$ , the sampling frequency  $f_s = 200 \text{ Hz}$ , the speed of vehicle  $c = 1.52322 \text{ m/s}$ , and the measurement bending moments number  $N_l = 7$ . Figure 3 plots the effect of  $BFN$  on the MOMA with Legendre basis function and one with Fourier basis function.

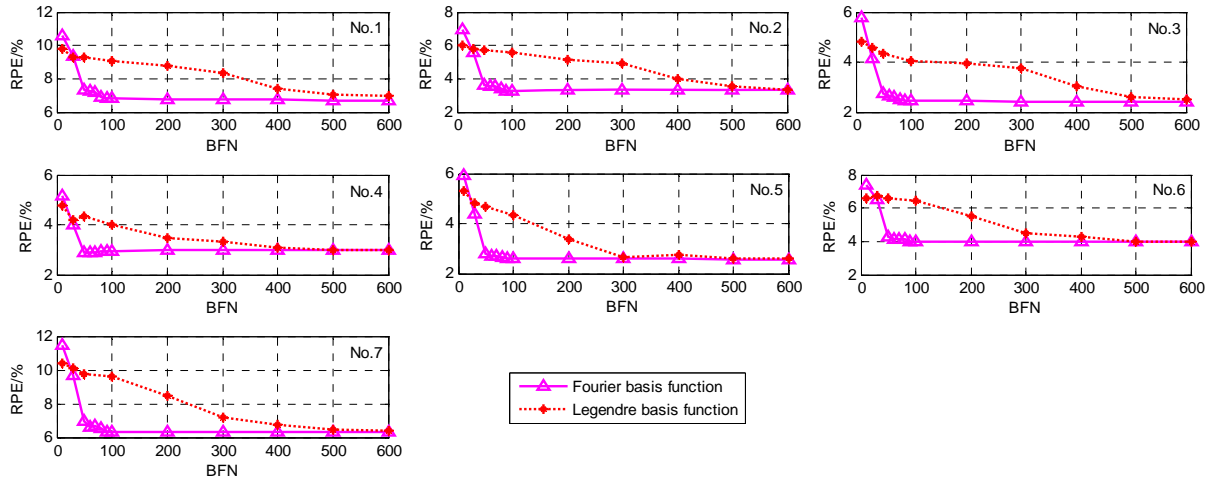


**Figure 3** - Effect of basis function number ( $BFN$ ) on MOMA

Figure 3 illustrates that both the  $RPE$  values tend to be reduced and finally to be close to each other when  $BFN$  increases. The major difference between them is that the rate of reduction is obviously different. If the Fourier basis functions are used, the  $RPE$  values are dramatically reduced to the lowest value and then kept the lowest constant after the basis function term is equal to about 100 or more for each case. However, for the Legendre basis functions, the corresponding basis function terms are increased up to be more than 400, even 500 for a stable solution.

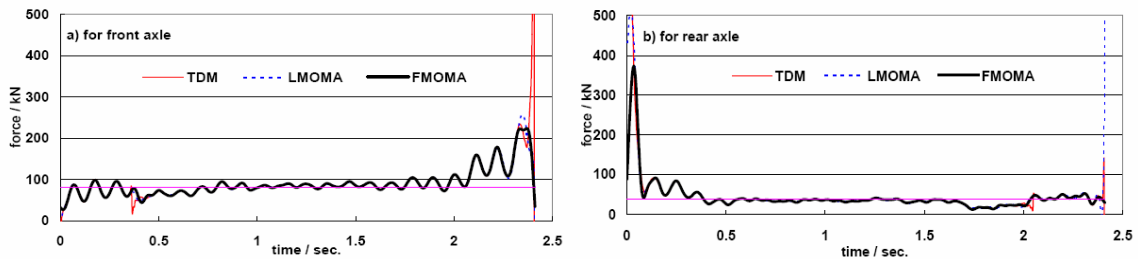


**Figure 4** - Comparison on moving force identified by TDM and MOMA



Figure 4 gives a comparison on the time histories of moving forces identified by the TDM and MOMA respectively when the basis function terms are equal to 500 for Legendre polynomials and 100 for Fourier series respectively. Here, the LMOMA is for the function of Legendre polynomials, the FMOMA for the function of Fourier series. It can be seen that the identified results from the MOMA are better than the TDM results, particularly for the moment at the beginning and the end of time history of two moving forces.

#### 4.2.3 Comparison on CPU execution time

**Table 3** - Comparison of CPU time (in second)

PART	TDM	MOMA
Forming coefficient matrix	18.219	19.907
Identifying forces	40.359	2.375
Rebuilding responses	1.063	1.094
<b>Total</b>	<b>59.641</b>	<b>23.376</b>

The case described here is of  $MN=4$ ,  $f_s=200\text{Hz}$ ,  $c=15$  Units,  $N_f=7$  using a computer with Intel Pentium (R) 4 CPU 2.6GHz 512MB RAM. The total sampling points for bending moment responses at each measurement station are 560 and the total sampling points for each wheel axle force are 483 in the time domain. A detail comparison of the CPU execution time for each part of the TDM and MOMA is listed in Table 3. It shows that both the MOMA and TDM take almost the same time for both of the rebuilding responses and forming the system coefficient matrix. However, the CPU execution time of MOMA is about 6% of TDM for the identifying force process. Hence, the total consuming time of MOMA is only two fifth of that of TDM. Therefore, MOMA is a better and fast method, whether from the point of view of identifying force time or from the total consuming time. This advantage with higher computation efficiency for the MOMA is especially valuable for the on-line real-time analysis of moving force identification in situ.

#### 4.2.4 Effect of Nyquist Fraction

In order to filter the high frequency noise of measured response signals, a Bessel IIR digital filter with low pass characteristics was chosen and implemented as a cascaded second order system. Different Nyquist fractions of the filter were chosen for the measured bending moments. The Nyquist fraction is defined as the ratio of cutoff frequency to sampling frequency of dynamic signals. A bigger Nyquist fraction indicates a filtered signal with higher frequency components in the frequency domain.

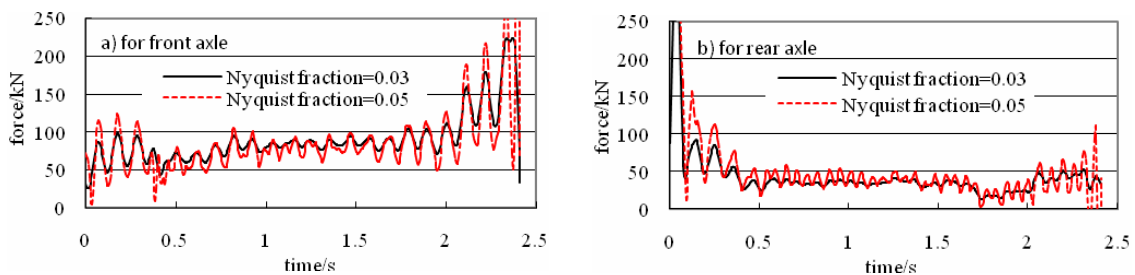


**Figure 5** - Effect of Nyquist fractions on moving force for MOMA

In this section, Nyquist fraction values were first set to 0.03 and 0.05 respectively and then used to filter the data samples recorded at the sampling frequency of 1000 Hz for all the cases. The new data sequence would be formed by sampling again at different rate, for example,  $f_s=200\text{Hz}$  as required, but others parameters  $MN=4$ ,  $c=15$  Units,  $N_5=7$  were not changed for each case. Figure 5 shows that the magnitude of identified forces increases and the identified forces have some clear higher frequency components when the Nyquist fraction has a higher value. Therefore, the Nyquist fraction should be selected properly to reasonably identify the moving vehicle loads on bridge.

#### 4.2.5 Effects of Different Solutions

If the parameters  $MN=4$ ,  $f_s=200\text{Hz}$ ,  $c=15$  Units,  $N_5=7$  were not changed for each case in this section, only two solutions, i.e. SVD and Regularization solutions, were adopted to solve the over-determined set of system equations respectively.

Figure 6 illustrates a comparison on the identified moving forces due to the two solutions for MOMA. Basically, the regularization results are in agreement with the SVD results except for the moment at the beginning and the end of time histories of moving forces as well as the moment at the accessing and exiting of vehicle. It shows that the fluctuation of identified moving forces can be effectively bounded at the moment mentioned above if the Regularization solution is adopted to solve the system equation for MOMA. The identified results by the Regularization solution are obviously improved. They are clearly better than the results by the SVD solution and more reasonable in practice.

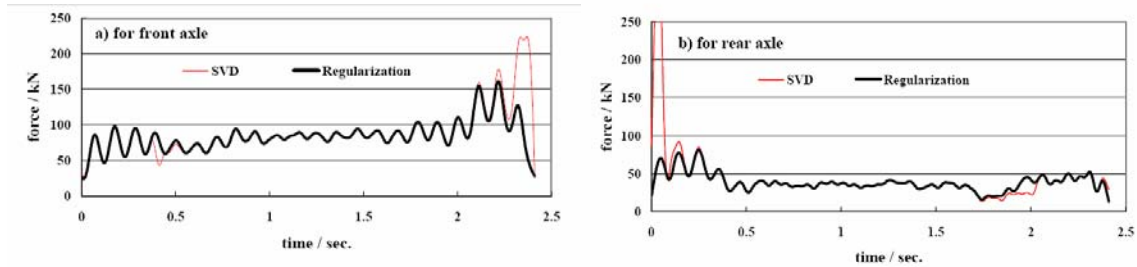


**Figure 6** - Effect of two solutions on moving forces for MOMA

## 5. Conclusions

In this paper, a MOM-based algorithm (MOMA) has been proposed for the identification of moving loads on bridges. Based on the numerical simulation and the experimental results, the following conclusions can be made. (1) The proposed MOMA is a successful method for the identification of moving loads from the responses induced by the moving vehicles on bridges. (2) The MOMA is obviously better than the existed TDM from all the aspects, especially for the constant load identification cases. (3) The MOMA can give satisfactory results with higher accuracy and computation efficiency when whether the SVD or regularization method is used. (4) The MOMA has robust immunity to the noise. It can improve the solutions of ill-posed problem to some extent. (6) The basis function terms play an important role in the MOMA. The different patterns and the number of basis function can lead to different computation efficiency, therefore, they should be properly selected and appropriately determined in order to keep the MOMA more effective. (7) The MOMA has

higher computation efficiency and better flexibility than the TDM. When the Fourier series are adopted as the basis function of the MOMA, the CPU execution time of MOMA is much less than the TDM. It is only about 6% of the TDM CPU execution time under the condition of keeping higher identification accuracy. The MOMA is obviously better than the TDM. To conclude, as a feasible and reasonable identification method, the MOMA should be firstly recommended as a practical method of moving force identification in situ.

## 6. Acknowledgments

The project is jointly supported by National Natural Science Foundation of China (50378009), the Key Project of Chinese Ministry of Education of China, the Foundation of Talent Program of Jinan University (51207052) and the Hong Kong Polytechnic University Postdoctoral Fellowship Research Grants (G-YX25).

## 7. Reference

- Ting E.C., and Yener M. (1983), Vehicle-Structure Interaction in Bridge Dynamic. *Shock Vib. Dig.*, 15(2), 3-9.
- Cantineni R. (1992), Dynamic behaviour of highway bridges under the passage of heavy vehicles. Swiss Federal Laboratories for Materials Testing and Research (EMPA) Report No. 220, 240 p.
- Heywood R.J. (1994), Influence of truck suspensions on the dynamic response of a short span bridge. *International Journal of Vehicle Design*.
- Peters R.J. (1984), A System to obtain vehicle axle weights. *Proceedings of 12th ARRB Conference*, 12, 10-18.
- Peters R.J. (1986), An unmanned and undetectable highway speed vehicle weighing system. *Proceedings of 13th ARRB and 5th REAAA Combined Conference Part 6*, 70-83.
- Chan T.H.T., and O'Conner C. (1990), Wheel Loads from Highway Bridge Strains: Field Studies. *ASCE Journal of Structural Engineering*, 116(7), 1751-1771.
- Yu L. (2002), Accounting for bridge dynamic loads using moving force identification system (MFIS). Hong Kong: The Hong Kong Polytechnic University.
- Chan T.H.T., Yu L. and Law S.S. and Yung T.H. (2001), Moving Force Identification Studies II: Comparative Studies. *Journal of Sound and Vibration*, 247(1), 77-95.
- Yu L. and Chan T.H.T. (2007). Recent research on Identification of moving loads on bridges. *Journal of Sound and Vibration*, 305(1-2):3-21.
- Jorgensen E, Volakis J L, Meincke P, and Breinbjerg O. (2004), Higher order hierarchical Legendre basis functions for electromagnetic modeling, *IEEE Transactions on Antennas and Propagation*, 52 (11), 2985-2995.
- Harrington R.F., (1968), *Field Computation by Moment Methods*. New York: Macmillan.